JOURNAL OF MATERIALS SCIENCE 30 (1995) 596–600

Mechanisms of char production from oxidized cellulose

F. J. NORTON, G. D. LOVE, A. J. MACKINNON, P. J. HALL
Department of Pure and Applied Chemistry, University of Strathclyde, 295 Cathedral Street, Glasgow G1 1XL, UK

A multi-technique approach, incorporating nuclear magnetic resonance (NMR), elemental analysis, differential scanning calorimetry (DSC), thermogravimetric analysis and surface-area determination, has been used to investigate the formation of chars by oxidized cellulose. It was found that oxidation of the cellulose tends to increase the surface area of the resulting char. NMR, elemental analysis and DSC show how cellulose oxidation tends to increase aromaticity and cross-linking. This, in turn, decreases diffusion rates of volatiles out of the oxidized cellulose during pyrolysis, giving denser carbons and higher BET surface areas.

1. Introduction

Activated carbons are an industrially important class of materials which are currently receiving renewed interest in such fields as pollution control, gas separation and as possible media for adsorbents in low-pressure methane-storage systems [1]. In many cases, especially where selective adsorption is required it is highly desirable to have carbon porosity with as narrow a distribution as possible. There have been many attempts to produce controlled-porosity carbons and a great variety of precursor materials and activation conditions have been used. In comparison, there have been relatively few studies that attempt to investigate in a systematic way the relationships between precursor material, pyrolysis and the properties of the resulting char. By paying more attention to the precursor and the effects of altering its structure on the carbon produced, it may be possible to produce a more uniform microporosity.

Cellulose derivatives in the form of biomass are the most common source materials for the production of active carbons. A wide variety of cellulose derivatives varying from coal, lignite, peat, wood through to agricultural waste products are used commercially [2]. The range of activation conditions and methods is equally wide using lower temperature chemical activation [3], higher temperature steam or CO_2 activation [2], or a combination of both.

Cellulose can be viewed as a linear condensation polymer consisting of D-anhydroglucopyranose units linked by β-1,4-glycosidic bonds [4]. The structure observed for the fully extended cellulose polymer is that of a flat ribbon with laterally protruding hydroxyl groups able to form both inter- and intra-molecular hydrogen bonds. Well-ordered areas of the cellulose structure contain hydrogen bonding between adjacent hydroxyl groups and the disordered areas show water bridging between adjacent chains [5]. The physical structure of cellulose has been studied using a variety of techniques including differential scanning calorimetry (DSC). The difficulty in finding a second-order phase transition in cellulose at a temperature lower than the onset of decomposition (~ 500 K), has been noted by Hatakeyama *et al.* [6].

There has long been interest in the partial oxidation of cellulose by chemical means through the use of different reagents, mainly as a means of preventing damage to the cellulose structure during processes such as textile fibre and wood pulp bleaching [4]. However, utilization of the product formed from physical oxidation through simple heating in an oxygen or air atmosphere of cellulose seems to have been somewhat neglected as a research field, probably because of its degrading effects on the cellulose polymer. The oxidation of alkali cellulose by gaseous oxygen in order to reduce the degree of polymerization of wood pulp for viscose rayon production, has been the major application of this type of oxidation process, with a controlled degradation of the polymer being desirable.

The production of active carbons generally involves pyrolysis of cellulose bases in a highly oxidizing environment with the result that the pyrolysis is performed on oxidized cellulose. To simplify the situation, it was decided to investigate the behaviour of pure cellulose and to decouple the processes of oxidation and pyrolysis in the production of chars.

The objective of the present work was to investigate the effects of preoxidation of pure cellulose on the nature of chars produced by pyrolysis in nitrogen. This is achieved by characterization of the fresh and oxidized cellulose by a variety of common polymer analytical techniques, solid state nuclear magnetic resonance (NMR), DSC and elemental analysis. Mass losses during pyrolysis of the fresh and oxidized cellulose was monitored by thermogravimetric analysis (TGA). Characterization of the resulting chars was by nitrogen adsorption at 77 K and BET analysis to yield surface area.

0022–2461

2. Experimental procedure

Cellulose powder ($< 20\ \mu m$) was obtained from the Aldrich Chemical Company and used as-supplied. Oxidation was performed at 473 K for varying times in a forced-circulation oven in air. Pyrolysis was performed in a tube furnace at 1173 K with a ramp rate of 10 K min^{-1} and 1 h dwell time in a flowing nitrogen atmosphere. The carrier flow rate was 1 l min^{-1} and the typical sample size ~ 5 g.

DSC was performed on a Mettler DSC 30 system. Temperature calibration was by the melting points of indium, lead and zinc standards. Temperatures are accurate to ± 0.5 K. Enthalpy calibration was by integrating the melting endotherm of an indium standard supplied by Mettler. It was estimated that enthalpies were accurate to $\pm 0.05\ J\ g^{-1}$. Standard aluminium pans were used with two pin holes to allow evaporation of water and the removal of pyrolysis products. The sample size was 10 mg. The polymer was spread in a monolayer over the base of the aluminium pans to maximize heat transfer to the cellulose. The procedure was as follows. The samples were dried *in situ* at 373 K for 30 min and then quenched to the starting temperature of 300 K. DSC was then performed at 10 K min^{-1} to a temperature of 523 K using a nitrogen carrier. The samples were again quenched to 300 K and DSC performed at 10 K min^{-1} to 523 K. The cycling procedure was repeated a further three times to identify only reversible phase changes in the samples.

25 MHz ^{13}C solid state NMR spectra of oxidized cellulose samples were obtained using a Bruker MSL 100 spectrometer equipped with a 7 mm double-bearing probe for cross-polarization (CP) and magic angle spinning (MAS). The samples were spun at a speed of 5 kHz, which is sufficient to reduce the side-band intensities to below 5% of those of the central aromatic bands in coals [7]. Typically, four thousand scans were accumulated with high-power ^1H decoupling in CP experiments employing a contact time of 2 ms and a recycle delay of 1.5 s. Dipolar dephasing was carried out on one sample to estimate the fraction of nonprotonated aromatic carbon present after oxidation. Delays of between 0 and 200 μs were introduced immediately before acquisition, during which the ^1H decoupler was switched off. Those carbons bound to hydrogen are rapidly dephased while non-protonated and rotationally mobile (methyl) carbon dephase more slowly. The attenuation of the non-protonated aromatic carbon signal with increasing dephasing time follows a single exponential law. Thus by plotting ln (aromatic signal area) versus dephasing time and extrapolating the best line fit through data in the region 60–200 μs to time zero, one can obtain an estimate of the fraction on non-protonated aromatic carbon. All FIDs were processed using exponential line-broadening factors of 20 Hz prior to Fourier transformation.

TGA was measured in a Stanton Redcroft TG750. A heating rate of 10 K min^{-1} was used and an air carrier. The typical sample size for TGA was ~ 10 mg.

Surface area determinations were made from nitrogen adsorption at 77 K with a BET analysis. Samples were outgassed *in situ* to 10^{-4} torr (1 torr = 133.322 Pa) at a temperature of 398 K for at least 12 h before the adsorption was determined volumetrically in a Micromeretics Accusorb 2100E machine.

TABLE I Ultimate analysis of fresh and oxidized cellulose

Sample	C (wt%)	H (wt%)	O (wt%)	H/C (g/g)	O/C (g/g)	Arom/aliph
Fresh	42.41	6.46	51.13	0.152	1.21	–
(C 100)	100	188	90			
24 h	43.30	6.64	50.34	0.154	1.17	0.152
(C 100)	100	184	87			
44 h	50.01	5.16	44.83	0.103	0.90	0.143
(C 100)	100	124	67			
50.5 h	51.27	4.64	44.09	0.090	0.86	0.106
(C 100)	100	108	64			
75 h	58.39	2.96	39.65	0.051	0.69	1.694
(C 100)	100	61	51			
165 h	53.64	2.86	43.50	0.053	0.81	4.341
(C 100)	100	60	61			
456 h	52.99	2.48	44.53	0.047	0.84	7.099
(C 100)	100	56	63			

3. Results and discussion

Table I shows the ultimate analyses of the cellulose following the oxidation procedure described above. The O/C ratio decreases rapidly between 24 and 75 h oxidation and then shows a slight increase up to 456 h. The initial decrease in oxygen content can be attributed to dehydration and, at the later stages of oxidation, loss of CO and CO_2 on de-polymerization of the cellulose. The slight increase in oxygen content between 75 and 456 h may be due to oxygen chemisorption on the cellulose. The H/C ratio decreases with an initial fast rate between 24 and 75 h oxidation followed by a slower rate of hydrogen loss with time of oxidation and appears to be approaching some limiting value.

Solid state ^{13}C NMR measurements were made to investigate further the chemical changes on oxidation. Fig. 1 shows the NMR measurements on the oxidized cellulose samples. The aromatic/aliphatic ratios were determined by integrating the aromatic and aliphatic peaks which are indicated in Fig. 1. The observed peaks were comparable to the accepted allocation of signals for cellulose: 70 p.p.m. = C-6, 80 p.p.m = C-2/C-3/C-5, 90 p.p.m = C-4, 110 p.p.m. = C-1 [8]. The unoxidized cellulose showed no significant aromatic functionality, which is consistent with the accepted structure of cellulose [2]. However, even relatively mild oxidation was sufficient to produce a small aromatic content. This was corroborated by a colour change from white in the unoxidized cellulose to light brown in the 24 h oxidized sample. The variation of the aromatic/aliphatic ratio with time of oxidation is shown in Fig. 2. Initially, the ratio decreased slightly from a value of 0.152 for 24 h oxidation to 0.106 following 50.5 h oxidation. The aromatic/aliphatic ratio then displayed a monotonic increase with time of oxidation up to 456 h.

The decrease in H/C values may be associated with initial dehydration (the O/C ratio decreased

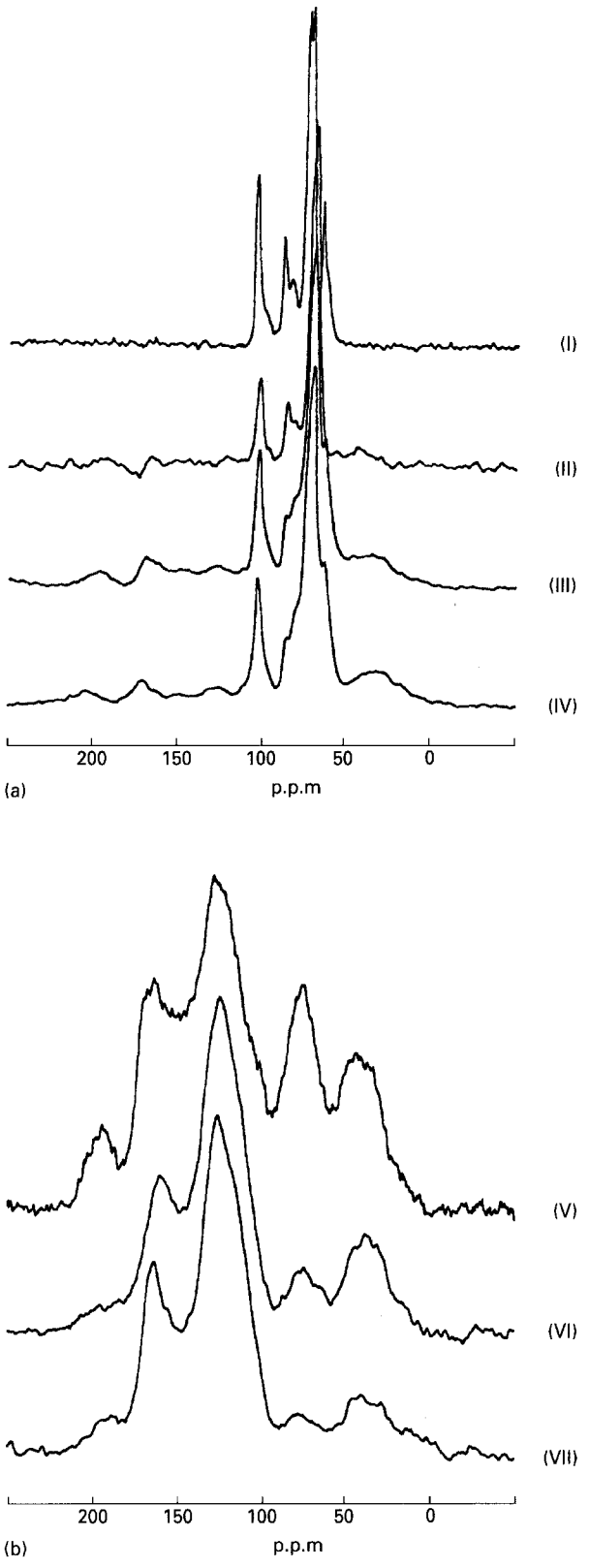

Figure 1 ^{13}C NMR for cellulose powder oxidized in air at 473 K for various times.

concurrently with H/C), accompanied by increasing aromaticity combined with the onset of crosslinking and more dehydration as the extent of oxidation increases. The variation of chemical composition based on C 100 together with the NMR data enables reasonable chemical structures to be constructed.

Fig. 2 shows that the initial decrease in H/C ratio cannot wholly be explained by simply an increase in

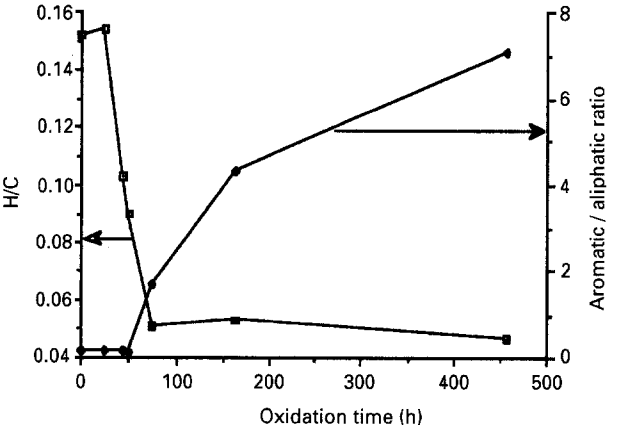

Figure 2 Variation of H/C ratio and aromatic/aliphatic ratio with time of oxidation in air at 473 K for cellulose powder. H/C values were derived from ultimate analysis and aromatic/aliphatic ratios from integration of the respective NMR peaks in Fig. 1.

aromaticity. In fact, the loss of hydrogen at this stage appears predominantly to be associated with an increase in cross-linkage of the cellulose combined with dehydration.

The initial slight decrease in overall aromaticity of the oxidized samples up to 50.5 h can be explained by the observed competitive generation of non-cellulose related aliphatics (at ~ 35 and 190 p.p.m.) in addition to the created aromatics (at ~ 128 and 162 p.p.m.). An early indication of possible carbon cross-linking taking place is seen after 24 h oxidation (Fig. 1a) when the C-6 signal (at ~ 70 p.p.m.) disappears. By 75 hours of oxidation, the cellulose structure has been completely altered (Fig. 1b) and the cellulose peaks have disappeared. The spectra at this stage consist of large aliphatic signals at 40 p.p.m., due to alkyl groups, and 80 p.p.m., due to ether groups, with a smaller aliphatic carbonyl signal at ~ 190 p.p.m. and aromatic peaks at 128 and 162 p.p.m. The newly generated aromatic peaks at 128 and 162 p.p.m. dominate the NMR plots after 165 h oxidation, with the new aliphatics at 40 and 80 p.p.m. taking a secondary role. The main aromatic peak centred at 128 p.p.m. corresponds to protonated and nonprotonated aromatics (possibly bridgeheads for cross-linking), and the smaller peak at 162 p.p.m. corresponds to phenolic aromatics and furan-type structures.

The general picture of changes on oxidation therefore appears to be an initial dehydration, occurring first at cellulose position C-6, with carbonyl production and generation of cross-links with some aromatic production. This is followed by significant aromatic production with cross-linking by a mixture of short aliphatic groups and ether linkages. In order to investigate the effects of these chemical changes on the physical structure, DSC was performed on the fresh and oxidized cellulose.

A typical DSC result, Fig. 3, for fresh cellulose shows a broad endotherm on run 1 from 330–400 K due to the evaporation of water which was present on the surface of the polymer. After this water has been removed it can be seen that there is a reversible second-order phase transition probably due to a glass to

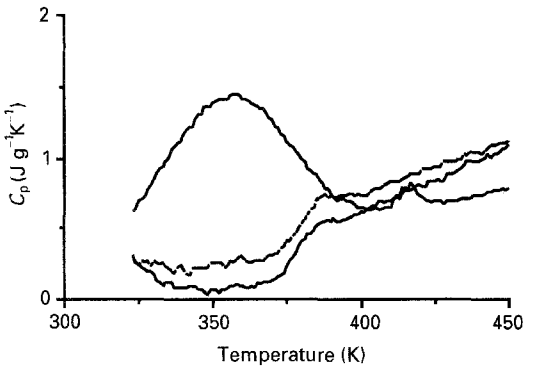

Figure 3 DSC plot for unoxidized cellulose powder cycled from 323–523 K in a nitrogen carrier. (—) Fresh run 1, (- - -) fresh run 2, (– – –) fresh run 3.

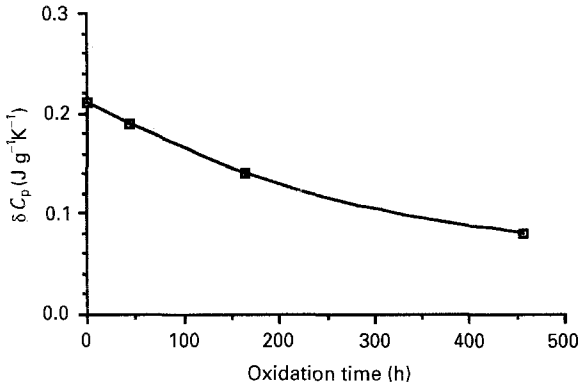

Figure 4 Variation of δC_P for the glass transitions of cellulose powder with time of oxidation in air at 473 K.

TABLE II Pyrolysis yields and carbon surface areas

Sample	Wt loss on oxidation (%)	Wt loss on carbonization (%)	Carbon yield (%)	BET SA (m^2g^{-1})
Fresh	–	81.6	18.4	65
200 °C, 24 h	9.9	80.2	17.8	360
200 °C, 44 h	38.3	69.9	18.6	415
200 °C, 50.5 h	44.3	67.9	17.9	420
200 °C, 75 h	65.4	57.4	14.7	459
200 °C, 165 h	76.2	59.5	9.6	507
200 °C, 456 h	72.7	59.4	11.1	541

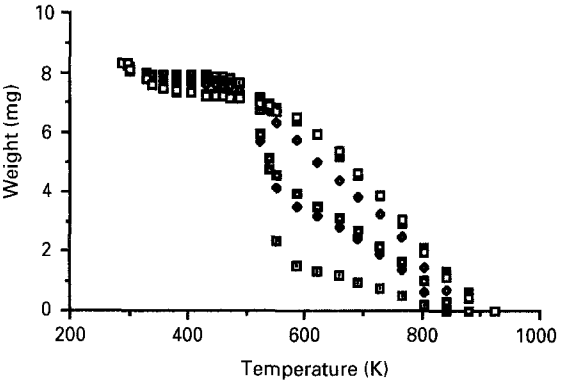

Figure 5 Thermogravimetric analysis in air for cellulose powder oxidized in air at 473 K for various times (⊡) 24 h, (◆) 44 h, (■) 50.5 h, (◆)75 h. (■) 165 h, (□) 456 h.

rubber transition in the region 370–380 K, which was obscured by the large evaporation endotherm. It has previously been observed by Hatakeyama *et al.* [6] that dry cellulose exhibits no phase transition at a temperature below that of decomposition. This disagreement could arise from the fact that our own DSC sensor is somewhat more sensitive than that of Hatakeyama *et al.*, [4]. Mackinnon *et al.* [9] have shown how sensor design can affect the detection of second-order phase transitions in coal. There were two effects of increasing oxidation on the glass transition behaviour of the cellulose. The first was that the temperature of the transition, T_g, increased with increasing oxidation. Such behaviour is usually associated with increasing cross-linkage or stiffening of the macromolecular chains. The other effect was in the intensities of the glass transitions. Fig. 4 shows the intensities of the glass transitions, δC_p, for the oxidized cellulose samples. δC_p's are defined conventionally. It was noted that the δC_p decrease with increasing extent of oxidation. Again, this may be due to an increase in cross-linking and density in the polymer which will make the structure considerably more rigid. The significance of this observation will be discussed shortly.

Table II shows the weight losses following oxidation and carbonization of the cellulose. The initial weight loss on oxidation up to 75 h is extensive, with the loss from 75–456 h being a lot smaller. The decomposition of cellulose in an oxygen atmosphere is well documented [10]. Initial weight loss is principally due to dehydration of water hydrogen bonded to the structure followed by dehydration of the actual cellulose structure, decarboxylation and general decomposition and depolymerization of the cellulose. The weight loss after 75 h being due mainly to hydrogen loss as the structure aromatizes with some loss of CO and CO_2. The carbon yields shown in Table II are the percentage of carbon in the original cellulose that remains in the char. The theoretical maximum carbon yield, if all of the carbon in the cellulose were converted into carbon in the char, is 68%. The char yield obtained for the untreated cellulose on carbonization at 1173 K using a heating rate of 10 K min^{-1} of 18.4% is comparable to that quoted by Brunner and Roberts [10]. Increasing the extent of oxidation decreases the overall carbon yield as more of the initial carbon in the cellulose structure is burnt away to form CO and CO_2 during the oxidation stage before carbonization.

Fig. 5 shows the TGA plots for the oxidized cellulose samples. The samples show slight weight loss from 300–500 K. This is probably due to loss of adsorbed H_2O. An increase in the oxidation period promotes greater weight loss in this temperature range from 300–500 K. This phenomenon can be explained by the presence of polar oxygen groups on the polymer surface of the more highly oxidized samples and hence, on heating in the TGA, these samples will subsequently show greater weight losses over the 300–500 K temperature range. The onset of pyrolysis can be observed for the samples after 500 K. Rapid weight loss can be observed for the fresh and more mildly oxidized samples probably due to depolymerization, and scission of C–O and C–C bonds within the

cellulose ring units, accompanied with evolution of more H_2O, CO and CO_2 [3]. The more highly oxidized samples lose weight less rapidly than the less oxidized cellulose. This is because an increase in oxidation period causes an increase in weight loss during the oxidation process due to the loss mainly of hydrogen and oxygen and some carbon and associated with this is an increase in cross-linking of the polymeric structure. Therefore, the more highly oxidized samples contain less volatile species and are, in fact, much strengthened by cross-linking and so will lose less weight during pyrolysis. Mass transfer through the more heavily cross-linked structure will also be slower, thus allowing more time for carbonization.

Table II shows the 77 K N_2 BET surface areas of the cellulose carbons. A clear trend can be seen whereby the surface area of the carbon increases with an increase in oxidation of the polymer precursor. The increase is an exponential rise which levels off at 456 h oxidation, with a surface area nearly nine times that of the fresh cellulose carbon.

To summarize, we believe that the different techniques applied to investigate changes to cellulose on oxidation, its subsequent pyrolysis and the properties of the resulting chars provide a better insight into how porosity forms in carbons during pyrolysis. NMR and elemental analysis show how oxidation increases aromaticity and cross-linking in the cellulose. This is confirmed from DSC measurements in changes in the second-order phase transitions of the oxidized cellulose. TGA shows that the increasingly oxidized cellulose exhibits less weight loss on pyrolysis and that the reactivity of the carbons decreases. The exact reasons for this are unclear but may be connected with the effectiveness of mass transfer through the matrix on pyrolysis. It is well established that lowering heating rates during the pyrolysis of carbonaceous materials tends to increase char yields. This is thought to be because the volatiles spend more time in the structure and hence produce more carbon. We believe a similar effect may be operating here. The more highly oxidized cellulose samples have greater aromaticity and TGA shows that they tend to decompose at high temperatures. Additionally, the reduction in δC_p indicates that there is less free volume and higher cross-linkage in the structure. This will also tend to decrease diffusion rates of volatiles out of the structure, thereby increasing char yields. The effect of increasing char yields is to produce denser carbons which contain more microporosity and therefore have higher surface areas.

4. Conclusions

Cellulose structure goes through radical changes on air oxidation at 473 K until, after 456 h the structure bears little or no resemblance to the original polymer. Initial oxidation promotes dehydration of the cellulose, resulting in some aromatic formation and cross-linking of the structure. Further oxidation encourages extensive aromatic production combined with increased cross-linking, resulting in a highly aromatic, highly cross-linked network with increased strength and resistance to weight loss. The extent of oxidation is linked to the surface area of the carbon produced from the cellulose precursors. Increased oxidation period produced carbons with higher N_2 BET surface areas. The fresh cellulose probably produces large pores with a generally open structure on carbonization, with the more highly oxidized cellulose developing a narrower porosity. The pre-oxidation procedure has been shown to be a good method for controlling the porosity of unactivated cellulose precursor carbons.

References

1. D. F. QUINN and J. A. MACDONALD, *Carbon* **30** (1992) 1097.
2. F. RODRIGUEZ-REINOSO and M. MOLINA-SABIO, *ibid.* **30** (1992) 1111.
3. M. JAGTOYEN and F. DERBYSHIRE, *ibid.* **31** (1993) 1185.
4. T. P. NEVELL and S. H. ZERONIAN, "Cellulose Chemistry and Applications" (Ellis Horwood, 1985).
5. "Cellulose: A review of the literature", Forestry Branch Departmental Publication no. 1201, (Ottawa, 1967).
6. T. HATAKEYAMA, K. NAKAMURA and H. HATAKEYAMA, *Polymer* **23** (1982) 1801.
7. J. A. FRANZ, R. GARCIA, J. C. LINEHAN, G. D. LOVE and C. E. SNAPE, *Energy Fuels* **6** (1992) 598.
8. M. BARDET, D, GAGNAIRE, R. NARDIN, D. ROBERT and M. VINCENDON, *Holzforschung* **40** (1986) 17.
9. MACKINNON *et al.*
10. T. P. NEVELL and S. H. ZERONIAN, in "Cellulose Chemistry and Applications", edited by F. Shafizadeh (Ellis Horwood, 1985)Ch. 11.
11. P. H. BRUNNER and P. V. ROBERTS, *Carbon* **18** (1990) 217.

Received 31 May
and accepted 27 July 1994